Support Care Cancer; 18: 1531-1538, 2010.

6) 深町勝巳、酒々井眞澄、徐結苟、津田洋幸. 発がん物質の中期代替検索法. FFI ジャーナル; 215: 390-397, 2010.

7) Sakamoto,Y., Nakae, D., Hagiwara, Y., Satoh, K., Ohashi, N., Fukamachi, K., Tsuda,H., Hirose, A., Nishimura,T., Hino, O., Ogata, A. Serum ERC/mesothelin level in rats with mesothelial proliferative lesions induced by multi-wall carbon nanotube. Journal of Toxicologic Sciences. 35: 265-270, 2010.

8) Tsuda, H., Futakuchi, M., Fukamachi, K., Shirai, T., Imaida, K., Fukushima, S., Tatematsu, M., Furukawa, F., Tamano S., Ito, N. A Medium-Term, Rapid Rat Bioassay Model for the Detection of Carcinogenic Potential of Chemicals. Toxicol Pathol. 38:182-187, 2010.

9) Xu, J., Futakuchi. M., Iigo, M., Fukamachi, K., Alexander, D.B., Shimizu.H., Sakai ,Y., Tamano,S., Furukawa, F., Uchino, T., Tokunaga, H., Nishimura, T., Hirose, A., Kanno, J., Tsuda, H. Involvement of macrophage inflammation protein 1 α (MIP1 α) in promotion of rat lung and mammary carcinogenic activity of nano-scale titanium dioxide particles administered by intra-pulmonary spraying. Carcinogenesis. 31:927-935, 2010.

10) Tsuda, H., Risk Assessment Studies of Nanomaterials in Japan and Other Countries. Asian Pacific J Cancer Prev,10, DIMS 30 th Anniverrsary Supplement. 11-12, 2010.

11) Xu, J., Sagawa, Y., Futakuchi, M., Fukamachi, K., Alexander, D. B., Furukawa, F., Ikarashi, Y., Uchino, T., Nishimura, T., Morita, A., Suzui, M., Tsuda, H. Lack of promoting effect of titanium dioxide particles on ultraviolet B-initiated skin carcinogenesis in rats. Food Chem Toxicol 49, 1298-1302, 2011.

12) Sadanandam, A., Futakuchi, M., Lyssiotis, C. A., Gibb, W. J., and Singh, R. K. A Cross-Species Analysis of a Mouse Model of Breast Cancer-Specific Osteolysis and Human Bone Metastases using Gene Expression Profiling. BMC Cancer 11, 304, 2011.

13) 広瀬明彦、高木篤也、西村哲治、津田洋幸、小縣昭夫、中江 大、樋野興夫、菅野 純「ナノマテリアルの慢性影響研究の重要性」YAKUGAKU ZASSHI 131 (2) : 195-201,2011

14) Sagawa, Y., Futakuchi, M., Xu, J., Fukamachi, K., Sakai, Y., Ikarashi, Y., Nishimura, T., Suzui, M., Tsuda, H., and Morita, A. Lack of promoting effect of titanium dioxide particles on chemically-induced skin carcinogenesis in rats and mice. The Journal of

toxicological sciences 37 : 317-327, 2012.

15) Takagi, A., Hirose, A., Futakuchi, M., Tsuda, H., and Kanno, J. Dose-dependent mesothelioma induction by intraperitoneal administration of multi-wall carbon nanotubes in p53 heterozygous mice. Cancer science 103: 1440-1444, 2012.

16) Ohba t, Sawada E, Suzuki Y, Yamamura, H, Ohya S & Imaizumi Y.Ca^{2+} influx facilitated by membrane hyperpolarization due to ATP-sensitive K^{+} channel openers enhances ciliary beating in mouse airway ciliated cells. J Pharmacol Exp Ther 投稿、改訂中。

17) Xu, J., Futakuchi, M., Shimizu H., Alexander, D.B., Yanagihara, K., Fukamachi, K., Suzui, M., Kanno, J., Hirose, A., Ogata, A., Sakamoto, Y., Nakae, D., Omori , T., and Tsuda , H. Multi-walled Carbon Nanotubes Translocate into the Pleural Cavity and Cause Hyperplasic Visceral Mesothelial Proliferation. Cancer Science. Vol.103 (12) :2045-2050, 2012.

18) Ohba t, Xu J, Sawada E, Suzuki Y, Tsuda H & Imaizumi Y. Interference of carbon-nanotubes on functional activities in primary cultured airway ciliary cells of the mice. 投稿準備中

19) Yabushita S, Fukamachi K, Tanaka H, Sumida K, Deguchi Y, Sukata T, Kawamura S, Uwagawa S, Suzui M, Tsuda H. Circulating MicroRNAs in Serum of Human K-ras Oncogene Transgenic Rats With Pancreatic Ductal Adenocarcinomas. Pancreas. ; 41(7):1013-8, 2012 Oct.

20) 吉岡智史、西村一彦、高村岳樹、酒々井眞澄、津田洋幸、板橋 豊 「キラル高速液体クロマトグラフィー/大気圧化学イオン化質量分析法によるグリシドール脂肪酸エステルの光学異性体分析」分析化学 Vol.61 (9) :783-790, 2012.

21) Masuda M, Toh S, Wakasaki T, Suzui M, Joe AK. Somatic evolution of head and neck cancer-biological robustness and latent vulnerability. Mol Oncol 7: 14-28, 2012.

22) Alexander DB, Iigo M, Yamauchi K, Suzui M, Tsuda H. Lactoferrin: an alternative view of its role in human biological fluids. Biochem Cell Biol 90: 279-306, 2012.

23) Fukamachi K, Tanaka H, Sakai Y, Alexander DB, Futakuchi M, Tsuda H, Suzui M. A novel reporter rat strain that expresses LacZ upon Cre-mediated recombination. Genesis 51: 268-74, 2013.

24) M. Futakuchi. Animal model of lung metastasis of hepatocellular carcinoma; A tool for the development of anti-

metastatic therapeutics. Journal of Cancer Therapy ; 4 420-425, 2013.

25) M. Futakuchi, R.K. Singh. Animal model for mammary tumor growth in the bone microenvironment. Breast cancer (Tokyo, Japan) , in press, 2013.

26) Xu J, Futakuchi M, Alexander DA, Fukamachi K, Numano T, Suzui M, Shimizu H, Omori T, Kanno J, Hirose A, Tsuda H. Nanosized zinc oxide particles do not promote DHPN-induced lung carcinogenesis but cause reversible epithelial hyperplasia of terminal bronchioles. Archives of Toxicology, in press, 2013.

27) Sakai Y, Fukamachi K, Futakuchi M, Hayashi H, Suzui M. Promotive effects of cell proliferation and chromosomal instability induced tribbles-related protein 3 in mouse mammary tumor cells. Oncol Rep 30 ; 64-70, 2013.

28) Yabushita S, Fukamachi K, Tanaka H, Fukuda T, Sumida K, Deguchi Y, Mikata K, Nishioka K, Kawamura S, Uwagawa S, Suzui M, Alexander DB, Tsuda H. Metabolomic and transcriptomic profiling of human K-ras oncogene transgenic rats with pancreatic ductal adenocarcinomas. Carcinogenecis, in press, 2013.

29) Yabushita S, Fukamachi K, Kikuchi F, Ozaki M, Miyata K, Sukata T, Deguchi Y, Tanaka H, Kakehashi A, Kawamura S, Uwagawa S, Wanibuchi H, Suzui M, Alexander DB, Tsuda H. Twenty-one proteins up-regulated in human H-ras oncogene transgenic rat pancreas cancers are up-regulated in human pancreas cancer. Pancreas, in press, 2013.

2. 学会発表

1) 五十嵐良明、瀧田葉子、相場友里恵、小濱とも子、内野　正、西村哲治. 反復経皮投与したナノサイズ酸化チタンの吸収性及び毒性について. 日本薬学会第 130 年会. 2010 年 3 月.

2) 二口充, 徐結苟, 飯郷正明, 深町勝巳, Alexander, D.B., 津田洋幸 (2010). ナノサイズ二酸化チタニウムの肺発がん促進作用のメカニズム. 第 99 回日本病理学会総会 東京, 2010 年 4 月 28 日.

3) 津田洋幸, 徐結苟, 二口充, 深町勝巳, 飯郷正明 (2010). ナノマテリアルのリスク評価ーアスベストから学ぶー. 第99回日本病理学会総会 東京, 2010年4月27日.

4) 五十嵐良明、相場友里恵、内野　正、西村哲治. 酸化チタンナノ粒子の

ラット皮膚透過性．第 37 回日本トキシコロジー学会学術年会 (2010. 7)

5) 津田洋幸、二口充、徐結苟、深町勝巳、酒々井眞澄．ナノ粒子の発がんリスク．第 17 回日本がん予防学会; 札幌: 2010 年 7 月 15 日.

6) Y. Ikarashi, Y. Aiba, Y. Takita, T. Uchino and T. Nishimura. Tissue distribution and toxicity of titanium dioxide nanoparticles in rats after repeated dermal exposure. XII International Congress of Toxicology (2010.7)

7) Nishimura, T., Kubota, R., Tahara, M., Obama, T., Sugimoto, N., Hirose, A., Ikarashi, Y. Bio-distribution of the fullerenes intravenous administrated. 2010 Annual meeting of the Korean Society of Environmental Health and Toxicology (2010.11)

8) Sawada E, Yamamura H, Ohya S, Imaizumi Y. Functional analysis of ion channels in murine airway ciliated cell. J. Pharmacol. Sci., Vol. 115, Suppl. 1, 80P. (2011) 第 84 回日本薬理学会抄録（2011 年 3 月 22-24 日横浜；学会自体は震災による影響で開催中止、ただし公式学会発表として抄録上で成立しているとの日本薬理学会の見解）

9) 深町勝巳、二口充、酒々井眞澄、徐結苟、津田洋幸．単層および多層カーボンナノチューブの肺発がん短期リスク評価．第 27 回日本毒性病理学会; 大阪: 2011 年 1 月 27 日.

10) 徐結苟、佐川容子、二口充、深町勝巳、五十嵐良明、西村哲治、古川文夫、内野正、酒々井眞澄、森田明理、津田洋幸．アレクサンダーダビィド．ナノ二酸化チタニウム粒子の皮膚発がん性修飾作用の欠如-ラットとマウスを用いた検討. 第 27 回日本毒性病理学会; 大阪: 2011 年 1 月 27 日.

11) 二口充、徐結苟、深町勝巳、酒々井眞澄、津田洋幸．ナノサイズ酸化亜鉛の吸入暴露による間質性肺炎の発生．第 27 回日本毒性病理学会; 大阪: 2011 年 1 月 27 日.

12) 徐結苟, 佐川容子, 二口充, 深町勝巳, 五十嵐良明, 西村哲治, 古川文夫, 内野正, 酒々井真澄, 森田明理, 津田洋幸 (2011). ナノ二酸化チタニウム粒子の皮膚発がん性修飾作用の欠如−ラットとマウスを用いた検討. 第27回日本毒性病理学会 大阪, 2011年1月28日.

13) 二口充, 深町勝巳, 徐結苟, 津田洋幸 (2010). 肺吸入曝露による発がんメカニズムにおいてナノ粒子の種類により異なる因子の関与. 第 26 回日本毒性病理学会学術集会 金沢, 2011 年２月３日.

14) Tsuda, H. (2010). Toxicologic Pathology of Nanomaterials. 28th International Congress of the International Academy of Pathology October, 10.

15) Tsuda, H., Xu, J., Futakuchi, M., Iigo, M., Fukamachi, K., Alexander, D.B., Nishimura, T., Hirose, A., and Kanno, J. (2010). Possible involvement of Macrophage inflammation protein 1alpha (MIP1alpha) in rat lung and mammary carcinogenesis induced by exposure to nano-scale titanium dioxide. STP/IFSTP 2010 Joint Symposium Chicago IL.

16) 津田洋幸, 二口充, 徐結苟, 深町勝巳, 酒々井真澄 (2010). ナノ粒子の発癌リスク. 第17回日本がん予防学会 札幌, 2011年7月16日.

17) 五十嵐良明、内野　正、西村哲治. 酸化チタンナノ粒子の皮膚感作性に及ぼす影響. 第 38 回日本トキシコロジー学会学術年会 (2011. 7)

18) 二口 充, 徐結苟, 深町勝巳, 酒々井眞澄, 津田洋幸. ナノサイズ酸化亜鉛の気管内噴霧による間質性肺炎の発生. 第38回日本トキシコロジー学会 横浜, 2011年７月11日.

19) 深町勝巳, 二口 充, 酒々井眞澄, 徐結苟, 津田洋幸. 単層および多層カーボンナノチューブのマクロファージを介した肺がん細胞増殖促進作用. 第38回日本トキシコロジー学会 横浜, 2011年7月12日.

20) 徐結苟、二口充、アレクサンダー・ダビッド、深町勝巳、坂井勇斗、酒々井眞澄、津田洋幸. ラット肺にカーボンナノチューブ投与による胸腔内粒子の検出および中皮細胞増殖の誘導. 第 70 回日本癌学会学術総会; 名古屋: 2011 年 10 月 3 日

21) 深町勝巳、坂井勇斗、二口充、津田洋幸、酒々井眞澄. 血清診断可能なラット肺がんモデル. 第 70 回日本癌学会学術総会; 名古屋: 2011 年 10 月 3 日

22) Futakuchi, M., Fukamachi, K., and Suzui, M. (2011). Soluble RANKL; significance of therapeutic target for tumor growth in the bone microenvironment. 70th Annual Meeting of the Japanese Cancer Association Nagoya.

23) 二口 充, 深町勝巳, 酒々井眞澄. 可溶性RANKL標的療法による骨微小環境での乳がん細胞の増殖および溶骨性変化の抑制とそのメカニズム. 第20回日本癌転移学会学術集会 浜松, 2011年11月17日.

24) Futakuchi, M., Fukamachi, K., and Suzui, M. (2011). Crosstalk between TGFbeta and AKT/PTEN signaling

pathway in the bone microenvironment : mechanism for tumor cell proliferation in the bone metastasis of breast cancer. The 16th Japan-Korea Cancer Research Workshop Sapporo.

25) 二口　充, 深町勝巳, 津田洋幸, 酒々井眞澄　骨微小環境における乳がん細胞の増殖に対する可溶性RANKLの治療標的分子としての意義. 平成23年度「個体レベルでのがん支援活動」ワークショップ　滋賀,　1月18日.

26) 酒々井眞澄、徐結苟、深町勝巳、二口充、菅野純、広瀬明彦、津田洋幸. 多層カーボンナノチューブ（CNT）の肺組織、細胞増殖および遺伝子発現への影響解析. 第28回日本毒性病理学会総会及び学術集会; 一橋: 2012年2月2日

27) 徐結苟、二口充、清水秀夫、David ALEXANDER、深町勝巳、柳原五吉、酒々井眞澄、菅野純、広瀬明彦、津田洋幸. 多層カーボンナノチューブ（MWCNT）の肺から胸腔内へ移行と中皮細胞の増殖. 第28 回日本毒性病理学会総会及び学術集会; 一橋: 2012年2月3日

28) 二口充、徐結苟、井上義之、高月峰夫、津田洋幸、酒々井眞澄. カーボンブラックの気管内噴霧により誘発された肺胞過形成様病変. 第 28 回日本毒性病理学会総会及び学術集会; 一橋: 2012年2月3日

29) 深町勝巳、二口充、徐結苟、井上義之、高月峰夫、津田洋幸、酒々井眞澄. フラーレンの気管内噴霧による肺発がん促進作用. 第 28 回日本毒性病理学会総会及び学術集会; 一橋: 2012年2月3日

30) 大羽輝弥、澤田英士、鈴木良明、山村寿男、大矢進、今泉祐治　「気管上皮繊維細胞における膜電位と細胞内カルシウム濃度の関係」　第８５回日本薬理学会年会　３月１６日　京都

31) 池永周平, 深町勝巳, 二口充, 酒々井眞澄. カーボンナノチューブ（CNT）の長さの違いによる肺組織への影響. 156回名古屋市立大学医学会例会, 2012年6月19日. 名古屋

32) 酒々井眞澄, 深町勝巳, 二口充, 森脇健太. 定量的構造活性相関によるパルミチン酸誘導体の抗がん活性スクリーニング. がん予防大会 2012 2012 年6月22日、23日、岐阜

33) 五十嵐良明、内野　正、西村哲治. ICP-MS によるカーボンナノマテリアルの金属の分析. 第39回日本トキシコロジー学会学術年会 ; 2012年7月

34) 沼野琢旬, 徐結苟, 二口充, 深町勝巳, 清水秀夫, 古川文夫, 酒々井真澄, 津田洋幸. ルチル型とアナターゼ型ナノサイズ二酸化チタニウム（TiO2）気管内噴霧によるラット肺組織に対する影響. 第39回日本毒性学会 2012年7月

17 日-19 日 仙台.

35) 深町勝巳、徐結苟、二口充、橋爪直樹、井上義之、高月峰夫、津田洋幸、酒々井眞澄. フラーレンの肺内噴霧による肺発がんプロモーション作用の検討. 第 39 回日本毒性学会学術年会; 仙台: 2012 年 7 月 18 日

36) 沼野琢旬、徐結苟、二口充、深町勝巳、清水秀夫、古川文夫、酒々井眞澄、津田洋幸. アナターゼ型ナノサイズ二酸化チタニウムの肺組織及び培養マクロファージへの影響ールチル型との比較検討ー. 第 39 回日本毒性学会学術年会; 仙台: 2012 年 7 月 18 日

37) 二口充、徐結苟、井上義之、高月峰夫、津田洋幸、酒々井眞澄. ナノサイズカーボンブラックの肺内噴霧により誘発された肺胞過形成. 第 39 回日本毒性学会学術年会; 仙台: 2012 年 7 月 18 日

38) 酒々井眞澄、徐結苟、深町勝巳、二口充、津田洋幸. 長さの異なる多層カーボンナノチューブの肺組織、細胞増殖および遺伝子発現への影響. 第 39 回日本毒性学会学術年会; 仙台: 2012 年 7 月 17 日

39) 池永周平, 深町勝巳, 二口充, 酒々井眞澄. 多層カーボンナノチューブ（CNT）の長さの違いにおける遺伝子発現への影響. 第 31 回分子病理学研究会 2012 年 7 月 22 日

40) 大羽輝弥、澤田英士、鈴木良明、山村寿男、大矢進、今泉祐治 「マウス気道上皮繊毛細胞運動の細胞内 Ca2+濃度及び膜電位への ATP 依存性 K^+チャネル開口薬の作用」 次世代を担う創薬・医療薬理シンポジウム 2012, 2012 年 9 月 1 日（神戸）

41) 池永周平, 深町勝巳, 二口充, 酒々井眞澄. 多層カーボンナノチューブ（MWCNT）の長さの違いにおける遺伝子発現への影響. 平成 24 年度がん若手研究者ワークショップ 2012 年 9 月 15 日

42) 深町勝巳、大嶋浩、二口充、津田洋幸、酒々井眞澄. ラット肺がんモデルにおける血清診断マーカー. 第 71 回日本癌学会学術総会; 札幌: 2012 年 9 月 20 日

43) 坂井勇斗、深町勝巳、二口充、林秀敏、酒々井眞澄. マウス乳がん細胞株を用いた pseudokinase TRB3 の機能解析. 第 71 回日本癌学会学術総会; 札幌: 2012 年 9 月 20 日

44) 池永周平、深町勝巳、二口充、津田洋幸、酒々井眞澄. カーボンナノチューブのラット肺組織、細胞増殖、遺伝子発現の影響. 第 71 回日本癌学会学術総会; 札幌: 2012 年 9 月 19 日

45) 二口充, 徐結苟, 井上義之, 高月峰夫, 津田洋幸, 酒々井真澄. カーボンブラックの気管内噴霧により誘発された肺胞過形成様病変. 第 29 回日本毒性病理学会 2013 年 1 月 31 日、2 月 1 日

46) 深町勝巳, 二口充, 徐結苟, 井上義之, 高月峰夫, 酒々井真澄, 津田洋幸. フラーレンの気管内噴霧による肺発がん

促進作用. 第 29 回日本毒性病理学会 2013 年 1 月 31 日、2 月 1 日

47) 酒々井眞澄, 徐結苟, 深町勝巳, 二口充, 菅野純, 広瀬明彦, 津田洋幸. 多層カーボンナノチューブ（CNT）の肺組織、細胞増殖および遺伝子発現への影響解析. 第 29 回日本毒性病理学会 2013 年 1 月 31 日、2 月 1 日

48) 深町勝巳、大嶋浩、二口充、津田洋幸、酒々井眞澄. ラット肺がんモデルにおける血清診断マーカー. 第 29 回日本毒性病理学会総会及び学術集会; つくば: 2013 年 1 月 31 日

49) 二口充、徐結苟、深町勝巳、津田洋幸、酒々井眞澄. ナノ材料の吸入暴露後、長時間経過して発生するリスクの背景となる肺組織の検索. 第 29 回日本毒性病理学会総会及び学術集会; つくば: 2013 年 1 月 31 日

50) 酒々井眞澄、沼野琢旬、深町勝巳、二口充、津田洋幸. 多層カーボンナノチューブの肺ばく露 2 週間および 52 週間経過後の影響. 第 29 回日本毒性病理学会総会及び学術集会; つくば: 2013 年 1 月 31 日

51) 柴田耕治、辻厚至、深町勝巳、二口充、津田洋幸、酒々井眞澄. Kras トランスジェニックラット膵がんモデルにおける画像診断の試み. 個体レベルのがん研究による相乗効果; 琵琶湖: 2013 年 2 月 7 日

52) 大羽輝弥、澤田英士、鈴木良明、山村寿男、大矢進、今泉祐治 「K_{ATP} チャネル開口薬によって引き起こされる膜電位の変化による繊毛運動への影響」第 86 回日本薬理学会年会 平成 25 年 3 月 23 日（福岡）

53) T. Numano, J. Xu, M. Futakuchi, K. Fukamachi, F. Furukawa, M. Suzui, H. Tsuda. Effect of anatase type nanosized titanium dioxide particles on the rat lung and cultured macrophage. American Association for Cancer Research Annual Meetting 2013; Washington DC: April 9, 2013.

54) M. Suzui, T. Numano, M. Futakuchi, K. Fukamachi. Evaluation of carcinogenic effect of multiwall carbon nanotubes on the rat lung at 2 and 52 weeks after pulmonary instillation. American Association for Cancer Research Annual Meetting 2013; Washington DC: April 9, 2013.

G. 知的所有権の取得状況（予定を含む）

1. 特許取得

PCT 出願

「アスベスト曝露マーカー及びその用途」

出願番号 PCT/JP2012/056321

2. 実用新案登録

該当なし

3. その他

該当なし

Ⅱ．研究成果の刊行に関する一覧表

書籍

著者名	論文タイトル	書籍全体の編集者名	書籍名	出版社名	出版地	出版年	ページ

雑誌

発表者氏名	論文タイトル名	発表誌名	巻号	ページ	出版年
Todo, H., Kimura, E., Yasuno, H., Tokudome, Y., Hashimoto, F., Ikarashi, Y., Sugibayashi, K.	Permeation pathway of macromolecules and nanospheres through skin.	Biol. Pharm. Bull	33	1394 -1399	2010
Uchino, T., Ikarashi, Y., Nishimura, T	Effects of coating materials and size of titanium dioxide particles on their cytotoxicity and penetration into the cellular membrane.	J. Toxicol. Sci.	36	95-100	2011
Naoi, K., Sunagawa, N., Morioka, T., Nakashima, M., Ishihara, M., Fukamachi, K., Itoh, Y., Tsuda, H., Yoshimi, N., Suzui, M.	Enhancement of tongue carcinogenesis in Hras128 transgenic rats treated with 4-nitroquinoline 1-oxide.	Oncol Rep.	23	337-344	2010
Masuda, M., Wakasaki, T., Suzui, M., Toh, S., Joe, A.K., Weinstein, I.B.	Stat3 orchestrates tumor development and progression: the Achilles' heel of head and neck cancers?	Curr Cancer Drug Targets.	10	117-126	2010
Ishihara, M., Iihara, H., Okayasu, S., Yasuda, K., Matsuura, K., Suzui, M., Itoh, Y.	Pharmaceutical interventions facilitate premedication and prevent opioid-induced constipation and emesis in cancer patients.	Support Care Cancer.	18	1531-1538	2010
深町勝巳、酒々井眞澄、徐結苟、津田洋幸.	発がん物質の中期代替検索法.	FFI ジャーナル	215	390-397	2010

Sakamoto,Y., Nakae, D., Hagiwara, Y., Satoh, K., Ohashi, N., Fukamachi, K., Tsuda,H., Hirose, A., Nishimura,T., Hino, O.,	Serum ERC/mesothelin level in rats with mesothelial proliferative lesions induced by multi-wall carbon nanotube.	Journal of Toxicologic Sciences.	35	265-270	2010
Tsuda, H., Futakuchi, M., Fukamachi, K., Shirai, T., Imaida, K., Fukushima, S., Tatematsu, M., Furukawa, F., Tamano S., Ito, N.	A Medium-Term, Rapid Rat Bioassay Model for the Detection of Carcinogenic Potential of Chemicals.	Toxicol Pathol.	38	182-187	2010
Xu, J., Futakuchi. M., Iigo, M., Fukamachi, K., Alexander, D.B., Shimizu.H., Sakai ,Y., Tamano,S., Furukawa, F., Uchino, T., Tokunaga, H., Nishimura, T., Hirose, A., Kanno, J., Tsuda, H.	Involvement of macrophage inflammation protein 1 α (MIP1 α) in promotion of rat lung and mammary carcinogenic activity of nano-scale titanium dioxide particles administered by	Carcinogenesis.	31	927-935	2010
Tsuda, H.	Risk Assessment Studies of Nanomaterials in Japan and Other Countries.	Asian Pacific J Cancer Prev.	10	11-12	2010
Xu, J., Saqawa, Y., Futakuchi, M., Fukamachi, K., Alexander, D.B., Furukawa, F., Tamano, S., Ikarashi, Y. Uchino, T., Nishimura, T., Morita, A., Suzui, M., Tsuda, H.	Lack of promoting effect of titanium dioxide particles on ultraviolet B-initiated skin carcinogenesis in rats.	Food Chem. Toxicol.	49	1298-1302	2011
Sadanandam, A., Futakuchi, M., Lyssiotis, C. A., Gibb, W. J., and Singh, R. K.	A Cross-Species Analysis of a Mouse Model of Breast Cancer-Specific Osteolysis and Human Bone Metastases using Gene Expression Profiling.	BMC Cancer	11 304		2011
広瀬明彦、高木篤也、西村哲治、津田洋幸、小縣昭夫、中江　大、樋野興夫、菅野　純	ナノマテリアルの慢性影響研究の重要性	YAKUGAKU ZASSHI 131	2	195-201	2011
Sagawa, Y., Futakuchi, M., Xu, J., Fukamachi, K., Sakai, Y., Ikarashi, Y., Nishimura, T., Suzui, M., Tsuda, H., and Morita, A.	Lack of promoting effect of titanium dioxide particles on chemically-induced skin carcinogenesis in rats and mice.	The Journal of toxicological sciences	37	317-327	2012

Takagi, A., Hirose, A., Futakuchi, M., Tsuda, H., and Kanno, J.	Dose-dependent mesothelioma induction by intraperitoneal administration of multi-wall carbon nanotubes in p53 heterozygous mice.	Cancer science.	103	1440-1444	2012
Ohba t, Sawada E, Suzuki Y, Yamamura, H, Ohya S & Imaizumi Y.	Ca^{2+} influx facilitated by membrane hyperpolarization due to ATP-sensitive K^{+} channel openers enhances ciliary beating in mouse airway ciliated cells.	J Pharmacol Exp Ther		投稿 改訂中	2012
Xu, J., Futakuchi, M., Shimizu H., Alexander, D.B., Yanagihara, K., Fukamachi, K., Suzui, M., Kanno, J., Hirose, A., Ogata, A., Sakamoto, Y., Nakae, D., Omori, T., and Tsuda, H.	Multi-walled Carbon Nanotubes Translocate into the Pleural Cavity and Cause Hyperplasic Visceral Mesothelial Proliferation.	Cancer Science.	103	2045-2050	2012
Ohba t, Xu J, Sawada E, Suzuki Y, Tsuda H & Imaizumi Y.	Interference of carbon-nanotubes on functional activities in primary cultured airway ciliary cells of the mice.			投稿 準備中	2012
Yabushita S, Fukamachi K, Tanaka H, Sumida K, Deguchi Y, Sukata T, Kawamura S, Uwagawa S, Suzui M, Tsuda H.	Circulating MicroRNAs in Serum of Human K-ras Oncogene Transgenic Rats With Pancreatic Ductal Adenocarcinomas.	Pancreas.	4 (7)	1013-1018	2012
吉岡智史、西村一彦、高村岳樹、酒々井眞澄、津田洋幸、板橋　豊	「キラル高速液体クロマトグラフィー/大気圧化学イオン化質量分析法によるグリシドール脂肪酸エステルの光学異性体分析」	分析化学	61 (9)	783-790	2012
Masuda M, Toh S, Wakasaki T, Suzui M, Joe AK.	Somatic evolution of head and neck cancer-biological robustness and latent vulnerability.	Mol Oncol	7	14-28	2012
Alexander DB, Iigo M, Yamauchi K, Suzui M, Tsuda H.	Lactoferrin: an alternative view of its role in human biological fluids.	Biochem Cell Biol	90	279-306	2012

Fukamachi K, Tanaka H, Sakai Y, Alexander DB, Futakuchi M, Tsuda H, Suzui M.	A novel reporter rat strain that expresses LacZ upon Cre-mediated recombination.	Genesis	51	268-274	2012
Futakuchi M.	Animal model of lung metastasis of hepatocellular carcinoma; A tool for the development of anti-metastatic therapeutics.	Journal of Cancer Therapy	4	420-425	2013
Futakuchi M, Singh RK.	Animal model for mammary tumor growth in the bone microenvironment.	Breast cancer (Tokyo, Japan)		in press	2013
Xu J, Futakuchi M, Alexander DA, Fukamachi K, Numano T, Suzui M, Shimizu H, Omori T, Kanno J, Hirose A, Tsuda H.	Nanosized zinc oxide particles do not promote DHPN-induced lung carcinogenesis but cause reversible epithelial hyperplasia of	Archives of Toxicology		in press	2013
Sakai Y, Fukamachi K, Futakuchi M, Hayashi H, Suzui M.	Promotive effects of cell proliferation and chromosomal instability induced tribbles-related protein 3 in mouse mammary tumor cells.	Oncol Rep	30	64-70	2013
Yabushita S., Fukamachi K., Tanaka H., Fukuda T., Sumida K., Deguchi Y., Mikata K., Nishioka K., Kawamura S., Uwagawa S., Suzui M., Alexander DB., and Tsuda H.	Metabolomic and transcriptomic profiling of human K-*ras* oncogene transgenic rats with pancreatic ductal adenocarcinomas.	Carcinogenesis		in press	2013
Yabushita S., Fukamachi K., Kikuchi F., Ozaki M., Miyata K., Sukata T., Deguchi Y., Tanaka H., Kakehashi A., Kawamura S., Uwagawa S., Wanibuchi H., Suzui M., Alexander DB., and Tsuda H.	Twenty-One Proteins Up-Regulated in Human H-ras Oncogene Transgenic Rat Pancreas Cancers are Up-Regulated in Human Pancreas Cancer.	Pancreas		in press	2013

III. 研究成果の刊行物・別刷

Permeation Pathway of Macromolecules and Nanospheres through Skin

Hiroaki TODO,[a] Eriko KIMURA,[a] Hirotaka YASUNO,[a] Yoshihiro TOKUDOME,[a] Fumie HASHIMOTO,[a] Yoshiaki IKARASHI,[b] and Kenji SUGIBAYASHI*[a,c]

[a] Faculty of Pharmaceutical Sciences, Josai University; [b] Life Science Research Centre, Josai University; 1–1 Keyakidai, Sakado, Saitama 350–0295, Japan; and [c] National Institute of Health Sciences; 1–18–1 Kamiyoga, Setagaya-ku, Tokyo 158–8501, Japan. Received February 15, 2010; accepted May 31, 2010; published online June 1, 2010

The permeation pathway of macromolecules and nanospheres through skin was evaluated using fluorescent isothiocyanate (FITC)-dextran (average MW, 4 kDa) (FD-4) and nanospheres (500 nm in diameter) in hairless rat abdominal skin and porcine ear skin as well as a three-dimensional cultured human skin model (cultured skin model). A low molecular hydrophilic compound, sodium fluorescein (FL) (MW, 376 Da), was used for comparison. FL penetrated the stratum corneum and permeated the viable epidermis of hairless rat skin, whereas less permeation of FL was observed through the cultured skin model, suggesting that the primary permeation pathway for the hydrophilic material may be skin appendages through the rat skin. A macromolecular compound, FD-4, was distributed through the hair follicles of the rat skin. In addition, nanospheres were detected in the hair follicles of porcine skin, although no skin permeation was detected. These findings suggest that appendage routes such as hair follicles can be a penetration pathway of macromolecules and nanospheres through skin.

Key words macromolecule; nanosphere; skin permeation pathway; transdermal drug delivery; hair follicle

Delivery of macromolecular compounds and nano-/microparticles has become more realistic due to the recent development of new tools and nanotechnologies for delivery enhancement.[1,2] The administration sites of such macromolecules and nano-/microparticles are supposed to be the mucosa, such as the gastrointestinal (GI) tract,[3] and ophthalmic, nasal and pulmonary[4] mucosa and skin.[5,6] Skin has been paid particular attention as an attractive administration site of these compounds because of its accessibility and easy application. Emulsion droplets, liposomes and other lipophilic carriers[7] containing small molecular active ingredients have already been investigated in the cosmetic field as well as therapeutic drug areas; however, the stratum corneum, the outermost layer of skin, has a primary function to protect the invasion and skin penetration of exogenous substances. Generally, only small molecular compounds less than 500 Da molecular weight are capable of significant passive permeation through the skin barrier (known as the 500 Dalton rule).[8] Thus, skin permeation of macromolecular compounds or nano-/microparticles is very difficult or impossible. Many reports have suggested that large molecules are likely to accumulate on the skin surface or appendages such as hair follicles.[9–12] Nevertheless, few reports have shown a quantitative approach for hair follicular penetration using quantitative skin permeation parameters.

Hairless rat and pig ear skins and three-dimensional cultured human skin model would be useful skin models with and without hair follicles, respectively, to clarify the contribution of hair follicles to skin permeation or the distribution of macromolecules and nanospheres.

In the present study, we selected fluorescent isothiocyanate (FITC)-dextran (average MW, 4 kDa) (FD-4) as a model macromolecular weight compound and 500 nm fluorescent polystyrene latex spheres as model nanospheres, and their potential for skin delivery was investigated by calculating skin permeation parameters or measuring the skin distribution of FD-4 and fluorescent polystyrene latex nanospheres in hairless rat abdominal skin and porcine ear skin as well as a three-dimensional cultured human skin model. Tables 1 and 2 summarize the model penetrant compounds and skin membranes used in this experiment. A low molecular hydrophilic compound, sodium fluorescein (FL) (MW 376 Da), was also used for comparison.

Theoretical Skin permeation kinetics is usually evaluated under an assumption that the skin consists of a single barrier membrane against drug permeation; however, generally, the drug-permeable membrane must be classed into three membranes: dissolution–diffusion membrane (Type 1 membrane), porous membrane (Type 2 membrane) and composite membrane (Type 3 membrane) of Type 1 and 2 membranes. Under the assumption that a single barrier of skin is one of these three membranes, the steady state skin permeation rate per unit application area, dQ/dt, is expressed using Fick's first law of diffusion as follows:

Type 1 membrane (dissolution–diffusion membrane)

$$\frac{dQ}{dt} = D \cdot \frac{K \cdot C_v}{L} = (KL)\left(\frac{D}{L^2}\right)C_v \quad (1)$$

Type 2 membrane (porous membrane)

$$\frac{dQ}{dt} = \frac{\varepsilon \cdot D_p}{\tau} \cdot \frac{C_v}{L} = (\varepsilon L)\left(\frac{D_p}{\tau L^2}\right)C_v \quad (2)$$

Type 3 membrane (composite membrane)

$$\frac{dQ}{dt} = (1-\varepsilon)\cdot D \cdot \frac{K \cdot C_v}{L} + \frac{\varepsilon \cdot D_p}{\tau} \cdot \frac{C_v}{L} = \left[(1-\varepsilon)KL\left(\frac{D}{L^2}\right) + (\varepsilon L)\left(\frac{D_p}{\tau L^2}\right)\right]C_v \quad (3)$$

where C_v is the initial concentration of the applied compound, D, K and L are diffusion coefficient, partition coefficient and barrier thickness of the membrane, respectively, and D_p, ε and τ are diffusion coefficients in water-filled pores, average fraction of diffusion area of pores, and tortuosity of the membrane, respectively. In examples 1 and 2, partition parameters and diffusion parameters of the pene-

* To whom correspondence should be addressed. e-mail: sugib@josai.ac.jp

trant are KL and DL^{-2} for the Type 1 membrane and εL and $D_p\tau^{-1}L^{-2}$ for the Type 2 membrane, respectively. The permeability coefficient, P, can be obtained as a product of the partition parameter and diffusion parameter. Diffusion lag time was obtained by dividing six by the diffusion parameter.

MATERIALS AND METHODS

Materials and Animals Both FL and FD-4 were obtained from Sigma-Aldrich Co., Ltd. (St. Louis, MO, U.S.A.). Fluorescent polystyrene latex nanospheres, Fluoresbrite® yellow green carboxylate microspheres (500 nm in average diameter), were purchased as model nanospheres from Polysciences, Inc. (Warrington, PA, U.S.A.). All other reagents and solvents were of reagent grade or HPLC grade, and used without further purification.

Male hairless rats (WBN/ILA-Ht, *ca.* 200—250 g) were supplied either from Life Science Research Center, Josai University (Sakado, Saitama, Japan) or Ishikawa Experimental Animal Laboratory (Fukaya, Saitama, Japan). Porcine ear skins were from Saitama Experimental Animal Laboratory (Sugito, Saitama, Japan). A three-dimensional cultured human skin model, Living Skin Equivalent-high (LSE-high), was obtained from Toyobo (Osaka, Japan).

Determination of *n*-Octanol–Water Partition Coefficient *n*-Octanol–water partition coefficient ($K_{o/w}$) of each fluorescent compound (FL or FD-4) was measured using distilled water–saturated *n*-octanol and *n*-octanol–saturated pH 7.4 phosphate buffered saline (PBS) at 32 °C. *n*-Octanol was added to the same volume of pH 7.4 PBS containing 10 mg/ml of each fluorescent, and the thoroughly mixed solution was equilibrated for 24 h. The aqueous phase was then analyzed using a fluorescence spectrophotometer (RF 5300PC; Shimadzu, Kyoto, Japan) at excitation and emission wavelengths of 490 and 520 nm, respectively. Logarithmic values of the partition coefficients are shown in Table 1.

***In Vitro* Skin Permeation Study** The skin permeation of FL and FD-4 was assessed using excised hairless rat abdominal skin and LSE-high. After the rats had been anesthetized by intraperitoneal injection of sodium pentobarbital (50 mg/kg), the abdominal skin was excised as described in our previous paper.[14] Stripped hairless rat skin was also used after removing the stratum corneum from the abdominal area by stripping 20 times with adhesive tape (Cellophane tape; Nichiban Co., Ltd., Tokyo, Japan). LSE-high was used after removing cultured skin pieces from the plastic insert with a knife. Each skin membrane was mounted in the side-by-side diffusion cell (effective diffusion area: 0.95 cm^2),[15,16] and 1.0 mM FL or 0.25 mM FD-4 (2.5 ml each) was applied to the stratum corneum side and the same volume of PBS was applied to the dermal side. Samples of 0.40 ml were taken periodically from the dermal side compartment, and then the same volume of the same solvent was added to keep the volume constant. FL or FD-4 concentration of each sample was determined using a fluorescence spectrophotometer, as explained above. The hairless rat skin and LSE-high surfaces were carefully rinsed with PBS several times to remove FL or FD-4 attached to the stratum corneum 6 h after starting the experiment. The obtained skin sample was embedded in Tissue-Tek® OTC compound (Miles, Inc., Elkhart, IN, U.S.A.) and stored at −80 °C until slicing.

Table 1. Physicochemical Properties of Model Compounds

Model compounds (abbreviation)	Molecular weight (Da)	Mean particle size or molecular radius	Log $K_{o/w}$ [a]
Sodium fluorescein (FL)	376	0.45 nm[13] (Stokes radius)	−0.615
FITC-dextran (FD-4)	4000	1.4 nm (Stokes radius)[13]	−0.773
Fluorescent polystyrene latex nanospheres (Fluoresbrite)	—	500 nm	—

a) $K_{o/w}$: *n*-octanol–water partition coefficient.

The skin permeation property of fluorescent polystyrene latex spheres (Fluoresbrite) was evaluated using excised hairless rat skin and excised porcine ear skin, which had been carefully shaved and the underlying excess fatty tissues removed from the dermis. LSE-high was also used to evaluate whether Fluoresbrite permeates the cultured skin. The obtained skin membranes were mounted in a Franz-type diffusion cell[14] (effective diffusion area: 1.77 cm^2). Then, 1.0 ml PBS-suspended solution containing Fluoresbrite (3.64×10^{10} particles/ml for 500 nm spheres) was applied to the stratum corneum surface, whereas 6.0 ml PBS was applied to the dermal side. The skin permeation test was performed at 32 °C over 12 h through hairless rat skin, porcine ear skin and LSE-high, while the receiver solution was continuously stirred with a star-head-type magnetic stirrer. The receiver solution was withdrawn 12 h after beginning the permeation experiment. The skins were then carefully rinsed with PBS several times to remove polystyrene spheres attached to the stratum corneum 12 h after starting the experiment. The obtained skin sample was embedded in Tissue-Tek® OTC compound (Miles, Inc., Elkhart, IN, U.S.A.) and stored at −80 °C until slicing.

All animal experiments were approved by the Institutional Animal Care and Use Committee of Josai University.

Evaluation of Skin Permeation Kinetics Steady-state flux was calculated by linear regression of the linear portion of normalized cumulative amount of penetrant permeated *versus* the time-curve (steady state; reached 4—6 h after starting the experiment), and the lag time was calculated from the intercept on the time axis by extrapolation from the steady state skin permeation profile. The normalized cumulative amount of penetrant permeated, Q_n, was calculated by dividing the cumulative amount permeated per unit area of skin by the initial concentration of the applied fluorescent compound in the donor compartment.[17] The permeation parameters were obtained by curve fitting the skin permeation data by Scheuplein's equation,[18] which comes from Fick's second law of diffusion. The least squares curve fitting method was performed using Microsoft® Excel Solver.[19] The calculation condition was 100 s for the calculation limit, 100 times for repeated calculation, 10^{-6} for accuracy, 5% basic tolerance and 10^{-3} for convergence. The pseudo-Newtonian method was used as an algorithm.

Sectioning of Hairless Rat Skin, Porcine Ear Skin and LSE-High Hairless rat skin, porcine ear skin and LSE-high embedded in Tissue-Tek® OTC compound were sequentially sliced with a cryostat (CM3050S; Leica, Wetzlar, Germany) to obtain horizontal and vertical 20 μm-thick sections. The prepared skin sections were observed with a fluorescence mi-

Table 2. Comparison of Skin Thickness and Presence or Absence of Hair Follicles in Several Skin Models

Skin model	Skin structure constitution	Stratum corneum thickness (μm)	Epidermis thickness (μm)	Whole skin thickness (mm)	Skin appendage	Relationship to human skin permeation
Hairless rat skin	Epidermis/dermis	15.4±3.3[20]	23.8±5.3[20]	0.86±0.06[20]	Yes	High
Pig skin	Epidermis/dermis	10.6±0.5	52.5±4.1	1.2±0.002	Yes	High
LSE-high	Epidermis/dermis	27.0±0.7	31.4±1.3	0.12±0.001	No	High

croscope (CK40; Olympus Corp., Tokyo, Japan).

Measurement of Thickness in LSE-High and Porcine Skin The thicknesses of the stratum corneum, epidermis, and whole skin in LSE-high and porcine skin were microscopically determined from microtomed sections after hematoxylin–eosin staining. Five good sections from each specimen were used to measure the stratum corneum, and whole skin thicknesses were measured by a light micrograph (IX71; Olympus Corp., Tokyo, Japan) and a calibrated ocular micrometer. The thickness of the epidermis was calculated by subtracting the stratum corneum thickness from the whole skin thickness. The thickness of hairless rat skin was cited from our previous paper.[20]

Observation of Skin Surface Shaved hairless rat and porcine ear skins were mounted with adhesive tape on a scanning microscopy (SEM) stage, and the skin surface was observed without coating by a low-vacuum SEM (S-3000N; Hitachi Ltd., Tokyo, Japan).

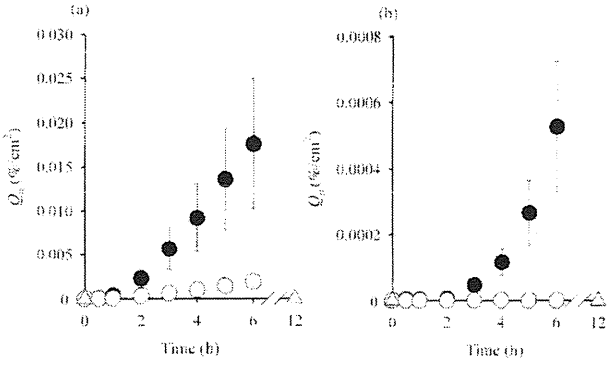

Fig. 1. Cumulative Amount of Hydrophilic Fluorescent Compounds, FL (●), FD-4 (○) and 500 nm Fluoresbrite (△) through Hairless Rat Skin (a) and LSE-High (b)

Normalized cumulative amount of the compounds permeating a percent per unit application area (%/cm^2)[17] was plotted on the vertical axis. Each data point represents the mean±S.E. of 3—4 experiments.

RESULTS

Many reports have shown that nano-/microspheres could not permeate the healthy stratum corneum.[21] In our study, therefore, the penetration pathway of hydrophilic fluorescent markers, FL and FD-4, was observed to evaluate the potential penetration of these mal-absorptive materials into skin and the delivery pathway through the skin barrier. The characteristics of model skin membranes (excised hairless rat skin, pig ear skin and LSE-high) are shown in Table 2. The stratum corneum in LSE-high was much thicker than the others. In addition, skin appendages such as sweat ducts and hair follicles could not be observed in LSE-high. Although many structural differences could be found between LSE-high and the others, and the permeation of several compounds (MW 122—236, $-1.5<\log K_{o/w}<2.1$) through LSE-high was about 10 times higher than through hairless rat and human skins, and the permeation rate through LSE-high showed a linear relationship to that through hairless rat and human skins.[14]

Figure 1a and b show the time course of the normalized cumulative amount of FL and FD-4 that permeated the unit area of excised hairless rat skin and LSE-high, respectively. In these experiments, 1.0 mM FL or 0.25 mM FD-4 (2.5 ml each) was applied to the skin surface to follow skin permeation. Interestingly, both fluorescent markers permeated hairless rat skin, whereas less permeation of FL and no permeation of FD-4 were observed through LSE-high. The Q_n of FL through hairless rat skin was 30-fold higher than through LSE-high.

The typical lag time and subsequent steady state permeation were observed for the permeation of both fluorescents through hairless rat skin. Permeability coefficients of FL and FD-4 were calculated by two methods using steady-state flux (observed value) and the curve fitting method (estimated value). These values are summarized in Table 3. The estimated vales were almost equal to the corresponding observed values and no significant differences appeared in hairless rat data. The calculated values of the permeability coefficient and Q_n of FL through LSE-high were about one-twelfth and one-thirtieth through hairless rat skin, respectively; furthermore, the lag time of FL through LSE-high (estimated value) was about three-fold of that through hairless rat skin. On the other hand, lag times of FL and FD-4 through hairless rat skin were almost the same as those through LSE-high.

Fluoresbrite was also applied to hairless rat skin and LSE-high. Although a Franz-type diffusion cell was used for measuring the skin permeation of Fluoresbrite, no permeation of the nanospheres was detected 12 h after starting the skin permeation experiment (see Fig. 1). No skin permeation was detected when Fluoresbrite was applied to porcine ear skin (data not shown).

Figure 2 shows fluorescent photographs illustrating the skin distribution of FL and FD-4 in hairless rat skin and LSE-high after topical application of these fluorescent markers. High-intensity FL was detected both in the stratum corneum and hair follicles of hairless rat (Fig. 2a), whereas FD-4 was mainly observed in the hair follicles (Fig. 2b). On the other hand, with LSE-high, FL was detected mostly in the stratum corneum and slightly in the viable epidermis (Fig. 2c) and FD-4 was found only on the skin surface (no skin penetration was observed for FD-4) (Fig. 2d). These results also suggest the high contribution of the transfollicular pathway to the transport of mal-absorptive hydrophilic compounds across the skin. In addition, this tendency was more

Table 3. Lag Time and Permeability Coefficients of FL and FD-4 through Excised Hairless Rat Skin or LSE-High

		FL		FD-4	
		Lag time (h)	Permeability coefficient (cm/s)	Lag time (h)	Permeability coefficient (cm/s)
Hairless rat	Estimated value[a]	2.0±0.16	$(1.1\pm0.5)\times10^{-8}$	2.2±0.01	$(3.6\pm0.2)\times10^{-9}$
	Observed value[b]	1.8±0.20	$(1.2\pm0.5)\times10^{-8}$	2.1±0.01	$(3.4\pm0.2)\times10^{-9}$
LSE-high	Estimated value[c]	5.4±0.4	$(9.4\pm2.4)\times10^{-10}$	—	$\ll1.21\times10^{-10.6}$
	Observed value[b]	—[c]	—[c]	—[c]	—[c]

a) Estimated value was calculated by curve-fitting the time course of the cumulative amount of skin permeation of compounds using Scheuplein's equation.[25] *b*) Observed value was obtained by the slope of steady-state flux and time-axis intercept of the time course of the cumulative amount of skin permeation of compounds. *c*) No steady state permeation was obtained until 6 h in the skin permeation study. *d*) Estimated value was calculated from lower quantitative limit of FD-4 in receiver cell 6 h after skin permeation study.

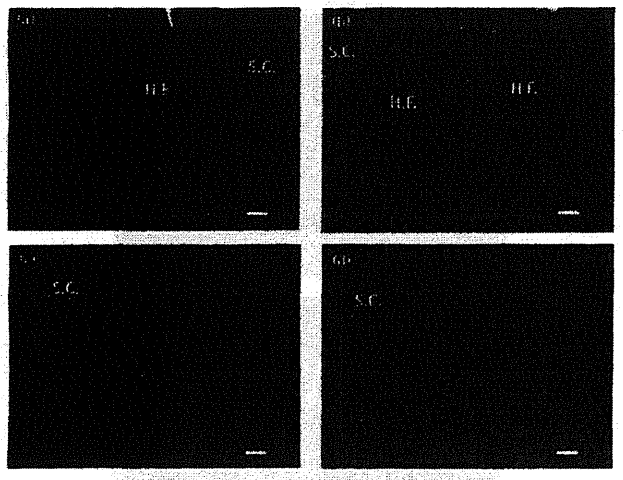

Fig. 2. Histological Observation of Hairless Rat Intact Skin (a, b) and LSE-High (c, d) after Application of FL (a, c) and FD-4 (b, d)

S.C.: Stratum corneum; H.F.: hair follicle. White burs=100 μm. (a, b): Fluorescence derived from FL or FD-4 was observed on the skin surface of skin and in hair follicles. (c, d): fluorescence derived from FL or FD-4 was observed in shallow areas or only on the surface, respectively, of LSE-high.

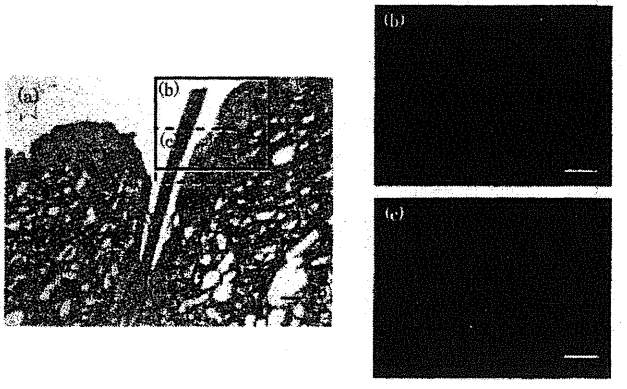

Fig. 3. Histological Observation of Excised Porcine Ear Skin 12 h after Application of 500 nm Fluoresbrite

a: Light micrograph of vertical slice. b and c: Fluorescent micrograph of area b and c in Fig. 3a. Bar=200 μm. (b, c): Fluoresbrite was observed in infundibulum of the hair follicle and surface of the hair shaft.

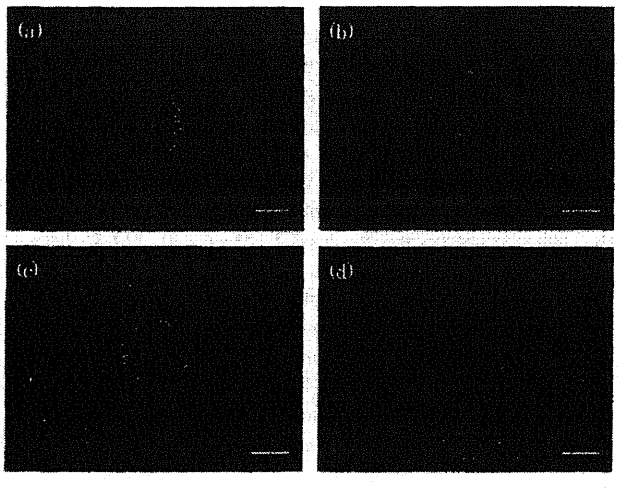

Fig. 4. Localization of 500 nm Fluoresbrite Penetrating the Hair Follicle

Fluorescence images (a—d) are horizontal slices at different depths from the skin surface of excised porcine ear skin 12 h after application of particles. a: *ca.* 20 μm, b: 40—60 μm, c: 80—100 μm, d: 200—220 μm. Bar=100 μm. (a): Fluoresbrite was detected on the surface of hair shaft and connective tissue in the follicle, (b, c): number of particles gradually decreased with an increase in depth from the skin surface, (d) only autofluorescence was observed.

marked when using the macromolecular compound. Thus, skin appendages such as hair follicles must be very important for the skin permeation of malabsorptive compounds.

Next, the skin distribution of Fluoresbrite (500 nm in diameter) was investigated after topical application to excised hairless rat skin, excised porcine ear skin and LSE-high. Nanospheres were detected only on the surface of the stratum corneum (data not shown) for hairless rat skin and LSE-high; therefore, a detailed observation was performed using excised porcine skin, since it has much larger hair follicles. Figure 3a shows a light microphotograph of porcine skin (vertical slice of hair follicle area) 12 h after the application of Fluoresbrite, and Figure 3b and c show fluorescent microphotographs of specific parts of the hair follicle area, as explained in Fig. 3a. Many nanospheres were found around the openings of the hair follicle, especially close to the epidermis side and around the hair shaft, as shown in Fig. 3b and c. The penetration depth of Fluoresbrite in the hair follicles was investigated by preparing horizontal slices of the hair follicle area of skin. The thickness of each skin section was adjusted to 20 μm. Figure 4 shows typical cross-section images of the hair follicle area from the skin surface (0—20 μm) to dermis side (200—220 μm) 12 h after application of Fluoresbrite to the excised porcine ear skin. In accordance with the photograph in Fig. 3, nanospheres could be detected in hair follicles, such as the surface of the hair shaft and connective tissue follicles, and the intensity due to nanospheres in the hair follicle gradually decreased with increasing pene-

tration depth; however, nanospheres could not be detected in connective tissue follicles below 200-μm depth from the skin surface. Only greenish-yellow autofluorescence derived from keratin and melanin was observed in Fig. 4d. This result clearly identified that the nanospheres were distributed or penetrated until about 100-μm depth, but did not penetrate as far as 200-μm depth from the skin surface 12 h after application. Thus, macromolecular compounds, such as FD-4 and nanospheres, are probably distributed or penetrate through the transfollicular pathway, although the extent is very marginal.

DISCUSSION

Three kinds of membranes are frequently utilized to describe the membrane permeation profiles of compounds, as explained in the theoretical section. In the dissolution–diffusion membrane (Type 1 membrane), compounds are dissolved and distributed into the membrane and then diffused in the homogeneous membrane. In the microporous membrane (Type 2 membrane), compounds are diffused across solvent (usually aqueous)-filled pores in the membrane. The third membrane (composite membrane) is the previous two membranes combined.

In the case of hairless rat and porcine skins, the stratum corneum and skin appendage may be the permeation pathway of compounds, especially for low molecular compounds ($\leq$500 Da). Thus, these animal skins would be assumed to be the third membrane. On the other hand, LSE-high would be classified as a dissolution–diffusion membrane, since three-dimensional cultured human skin model has no appendages, such as hair follicles and sweat ducts.

Although LSE-high is such a skin appendage-deficiency model, it was observed in our previous study[14] that logarithmic values of the permeability coefficient, $\log P$, of seven drugs through LSE-high were fairly proportional to those through excised hairless rat, pig and human skins, and the partition parameters of LSE-high were almost the same as in other skins. For FL and FD-4 applied to LSE-high, low permeation and no permeation were observed in the present study, while permeation through hairless rat skin was observed. The permeability coefficient, P, of FD-4 through LSE-high was calculated from the lower quantitative limit of FD-4 in receiver solution (Table 3). The estimated value was about thirtieth of that of FD-4 through hairless rats. FL (pK_a 1: 4.32, pK_a 2: 6.5)[22] predominantly exists as an ionized form in pH 7.4 PBS, and FD-4 has a high molecular weight; therefore, the P-value of FL and FD-4 through LSE-high was much lower than through hairless rat skin.

The P-value is a product of the partition parameter (KL or εL) and diffusion parameter (DL^{-2} or $D_p\tau^{-1}L^{-2}$).[23] To clarify the differences of skin permeation profiles between hairless rat skin and LSE-high, the partition parameter and diffusion parameter were compared.

Table 4 shows the partition and diffusion parameters, which were calculated from curve-fitting the time course of the cumulative amount of FL and FD-4 permeating hairless rat skin and LSE-high. Interestingly, both parameters of LSE-high calculated from FL permeation were not the same as those of hairless rat skin. These differences might reflect the different permeation routes of FL between these skins.

Table 4. Comparison of Partition Parameter and Diffusion Parameter between Hairless Rat Skin and LSE-High

Compound	Membrane	Partition parameter (KL or εL) (cm)	Diffusion parameter (DL^{-2} or $D_p\tau^{-1}L^{-2}$) (s^{-1})
FL	Hairless rat	$(4.7\pm1.8)\times10^{-4}$	$(2.3\pm0.18)\times10^{-5}$
	LSE-high	$(1.1\pm0.31)\times10^{-4}$	$(8.6\pm0.75)\times10^{-6}$
FD-4	Hairless rat	$(1.7\pm0.13)\times10^{-4}$	$(2.0\pm0.06)\times10^{-5}$
	LSE-high	—	—

KL and DL^{-2} or εL and $D_p\tau^{-1}L^{-2}$ were calculated by curve-fitting the skin permeation profile of FL and FD-4 through hairless rat skin and LSE-high.

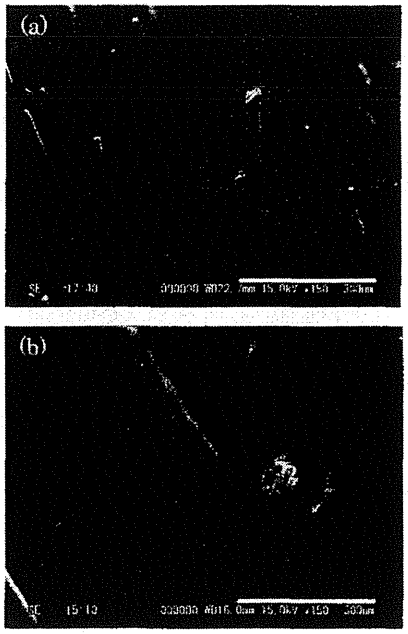

Fig. 5. SEM Observation of Hairless Rat Skin (a) and Porcine Ear Skin (b)

Bar=300 μm.

Increased partition and diffusion parameters of FL in hairless rat skin might mean that FL was mainly partitioned in pore routes and permeated the pore routes of skin; therefore, skin appendages, such as hair follicles, are the predominant permeation route of FL.

The diffusion parameters of FL and FD-4 in hairless rat skin showed almost the same value due to the slight difference in the cubic root of the molecular weight of these compounds, because the diffusion coefficient is proportional to the reciprocal of the cubic root, which is given by the Stokes–Einstein equation. Therefore, FL and FD-4 must permeate through almost the same permeation pathway of skin. On the other hand, the partition parameter of FD-4 was about one-third that of FL, indicating that FD-4 permeated skin through a more restricted pathway, such as hair follicles, than the FL pathway. In addition to this assumption, the present fluorescence images strongly supported the skin appendage route as a useful pathway for skin permeation and/or the distribution of such macromolecular compounds.

Fluoresbrite did not permeate hairless rat skin or LSE-high. Thus, porcine skin was selected to observe its skin distribution because the pores of hair follicles in porcine skin

are larger than in hairless rat skin (see Fig. 5). Fluoresbrite was especially observed in the infundibulum of hair follicles of porcine skin and no spheres were observed more than 100-μm depth from the skin surface (Fig. 4). It is reasonable that Fluoresbrite was detected only in the hair follicle because even FD-4, having a smaller molecular radius than nanospheres, was mainly detected in hair follicles.

This indicated that hair follicles are expected to be a useful pathway, not only for macromolecular compounds, but also nanospheres, through the skin barrier. Scheuplein[18] reported that the contribution of the transappendage route to the skin permeation of low molecular compounds must be very low, although the transfollicular pathway would play a very important role in the early stage of skin permeation and distribution. This is because the skin appendage area is only 0.1% of the total skin surface area.[18,24] Further study is necessary to fully elucidate the contribution of hair follicles to the skin permeation or distribution of hydrophilic compounds and nano-/microspheres. This contribution of hair follicles can be assessed using skin permeation parameters, such as $\varepsilon \cdot L$ and $D/\tau \cdot L^2$ as above.

CONCLUSION

The present study revealed that important role of hair follicles as a permeation pathway or distribution pathway for hydrophilic compounds and nanospheres. Although not only skin features, such as hair density and follicle size, but also physicochemical properties, such as molecular size and *n*-octanol/water partition coefficient of compounds, affect their transfollicular permeation,[25] analysis of the hair follicle contribution to the overall skin permeation of compounds using permeation parameters will help to understand efficient compound targeting of hair follicles.

Acknowledgement This study was supported by a Grant-in-Aid for Scientific Research (H20-iyaku-ippan-001) from the Ministry of Health, Labor, and Welfare, Japan.

REFERENCES

1) Ravi Kumar M. N., *J. Pharm. Pharm. Sci.*, **3**, 234—258 (2000).
2) Bilati U., Allemann E., Doelker E., *Eur. J. Pharm. Biopharm.*, **59**, 375—388 (2005).
3) Takeuchi H., Matsui Y., Sugihara H., Yamamoto H., Kawashima Y., *Int. J. Pharm.*, **303**, 160—170 (2005).
4) Todo H., Iida K., Okamoto H., Danjo K., *J. Pharm. Sci.*, **92**, 2475—2486 (2003).
5) Alvarez-Roman R., Naik A., Kalia Y. N., Guy R. H., Fessi H., *J. Controlled Release*, **99**, 53—62 (2004).
6) Almeida A. J., Souto E., *Adv. Drug Deliv. Rev.*, **59**, 478—490 (2007).
7) Honeywell-Nguyen P. L., Wouter Groenink H. W., Bouwstra J. A., *J. Liposome Res.*, **16**, 273—280 (2006).
8) Bos J. D., Meinardi M. M., *Exp. Dermatol.*, **9**, 165—169 (2000).
9) Lademann J., Weigmann H., Rickmeyer C., Barthelmes H., Schaefer H., Mueller G., Sterry W., *Skin Pharmacol. Appl. Skin Physiol.*, **12**, 247—256 (1999).
10) Toll R., Jacobi U., Richter H., Lademann J., Schaefer H., Blume-Peytavi U., *J. Invest. Dermatol.*, **123**, 168—176 (2004).
11) Trauer S., Patzelt A., Otberg N., Knorr F., Rozycki C., Balizs G., Buttemeyer R., Linscheid M., Liebsch M., Lademann J., *Br. J. Clin. Pharmacol.*, **68**, 181—186 (2009).
12) Teichmann A., Jacobi U., Ossadnik M., Richter H., Koch S., Sterry W., Lademann J., *J. Invest. Dermatol.*, **125**, 264—269 (2005).
13) Mota M. C., Carvalho P., Ramalho J., Leite E., *Int. Ophthalmol.*, **15**, 321—326 (1991).
14) Watanabe T., Hasegawa T., Takahashi H., Ishibashi T., Takayama K., Sugibayashi K., *Altern. Animal Test Experiment.*, **8**, 1—14 (2001).
15) Okumura M., Sugibayashi K., Ogawa K., Morimoto Y., *Chem. Pharm. Bull.*, **37**, 1404—1406 (1989).
16) Obata Y., Takayama K., Maitani Y., Machida Y., Nagai T., *Biol. Pharm. Bull.*, **16**, 312—314 (1993).
17) Sugibayashi K., Hosoya K., Morimoto Y., Higuchi W. I., *J. Pharm. Pharmacol.*, **37**, 578—580 (1985).
18) Scheuplein R. J., *J. Invest. Dermatol.*, **48**, 79—88 (1967).
19) Sugibayashi K., Hayashi T., Matsumoto K., Hasegawa T., *Drug Metab. Pharmacokinet.*, **19**, 352—362 (2004).
20) Sato K., Sugibayashi K., Morimoto Y., *J. Pharm. Sci.*, **80**, 104—107 (1991).
21) Scientific Committee on Consumer Product, "Opinion on Safety on Nanomaterials in Cosmetic Products," 2007.
22) Lauer A. C., Lieb L. M., Ramachandran C., Flynn G. L., Weiner N. D., *Pharm. Res.*, **12**, 179—186 (1995).
23) Okamoto H., Yamashita F., Saito K., Hashida M., *Pharm. Res.*, **6**, 931—937 (1989).
24) Ogiso T., Shiraki T., Okajima K., Tanino T., Iwaki M., Wada T., *J. Drug Target.*, **10**, 369—378 (2002).
25) Knorr F., Lademann J., Patzelt A., Sterry W., Blume-Peytavi U., Vogt A., *Eur. J. Pharm. Biopharm.*, **71**, 173—180 (2009).